

## Crystal-melt interfacial free energies of hard-dumbbell systems

Yan Mu and Xueyu Song

*Department of Chemistry, Iowa State University, Ames, Iowa 50011, USA*

(Received 19 May 2006; revised manuscript received 2 September 2006; published 29 September 2006)

The crystal-melt interfacial free energies of different crystal orientations and crystal forms for the hard-dumbbell systems have been calculated directly using a multistep thermodynamic perturbation method via nonequilibrium work measurements with a cleaving procedure. We found that for the plastic crystal phase, the interfacial free energies decrease as the reduced bond length  $L^*$  increases and the anisotropy is very weak as in isotropic systems. On the other hand, for the orientationally ordered crystal phase, the interfacial free energies become more than three times larger and the anisotropy is about 13%. These results may have significant implications for our understanding on the nucleation kinetics in molecular systems and the search of optimal conditions of protein crystallization.

DOI: [10.1103/PhysRevE.74.031611](https://doi.org/10.1103/PhysRevE.74.031611)

PACS number(s): 68.08.-p, 64.10.+h

The crystal-melt interfacial free energy  $\gamma$  is of significant importance in the nucleation and crystal growth. Both its magnitude and anisotropy are primary physical parameters governing the kinetics and morphology of crystal growth [1]. In recent years, much effort has been made on the measurements and predictions of this quantity with experimental, theoretical, and computer simulation methods.

Experimentally,  $\gamma$  is mainly estimated through measurements of crystal nucleation rates [2–5]. Direct measurements are difficult and so far only a few materials have been studied via Wulff construction [6,7]. However, the values of  $\gamma$  obtained by measuring crystal nucleation rates are not very accurate due to the approximations inherent in the classical nucleation theory. Theoretically, the basic approach of calculating the crystal-melt interfacial free energy has been the density-functional theory (DFT) [8–11]. Unfortunately, the results from the DFT method are highly dependent on the approximations used and the density profile parametrizations employed in the DFT studies. Moreover, it is very difficult to resolve the anisotropy of the interfacial free energies with the DFT method [11].

Thus computer simulations will be very useful alternatives to provide reliable information on the crystal-melt interfaces and their interfacial free energies. In recent years, two main simulation methods are developed: capillary-wave method [12–19] and thermodynamic integration with a cleaving procedure [20–25]. The capillary-wave method is relatively accurate in determining the anisotropy of the interfacial free energies. However, it is difficult for this method to provide very accurate values of  $\gamma$  [18]. Alternatively, the crystal-melt interfacial free energy per unit area is defined as the reversible work required to form a unit area of the interface, which can be created through a cleaving procedure. However, it is very time consuming for the thermodynamic integration method to avoid hysteresis, and in certain situations hysteresis is large and persistent and it is difficult to eliminate such hysteresis. Recently, we have developed a multistep thermodynamic perturbation method to compute the interfacial free energies by nonequilibrium work measurements with a cleaving procedure [25]. This new methodology has overcome some of the difficulties of using thermodynamic integration and thus opens the door to calculate interfacial free energies of more complex systems.

So far, the crystal-melt interfacial free energies for systems with isotropic potentials, such as a hard-sphere system [18,21,24], Lennard-Jones systems [17,20,22,25], or metallic systems [12,13,15,16], have been investigated extensively. For systems with anisotropic potentials, only the interfacial free energy of the plastic crystal system, which has similar behaviors as the spherical systems, was studied recently [19]. However, to the best of our knowledge, there are no studies yet on the estimation of the magnitude nor the anisotropy of the crystal-melt interfacial free energy for an orientationally ordered crystal system, which is qualitatively different from isotropic systems. Such information is not only useful for our understanding of the nucleation kinetics of molecular systems, but also has practical implications for the search of optimal conditions of protein crystallization [26,27]. Therefore, reliable estimations of the magnitude and the anisotropy of the crystal-melt interfacial free energies for such systems with anisotropic potentials are highly desirable. However, both the capillary-wave method and thermodynamic integration with a cleaving procedure become invalid to calculate such quantities for the case of the orientationally ordered crystal phase. On the one hand, the interface between the orientationally ordered crystal and its melt is faceted and the interfacial fluctuations cannot be measured. On the other hand, there exists a large hysteresis between the forward and reverse paths using a traditional thermodynamic integration method with a cleaving technique. Thus our newly developed multistep thermodynamic perturbation method [25] provides a practical way for such calculations.

In this paper, we have used this method to compute the crystal-melt interfacial free energies of different crystal orientations for orientationally disordered and orientationally ordered hard-dumbbell systems by nonequilibrium work measurements with a cleaving procedure. For the hard-dumbbell systems, there are two kinds of basic crystal structures: orientationally disordered fcc plastic crystal (PC) and orientationally ordered crystal (OOC). In the current work, one of the OOC structures CP1 is considered as a detailed phase diagram existed both from simulations and DFT calculations [28–31]. Figure 1 shows the two hard-dumbbell crystal structures and the notations of crystal directions used in this paper.

The system potential of hard-dumbbell systems is taken as

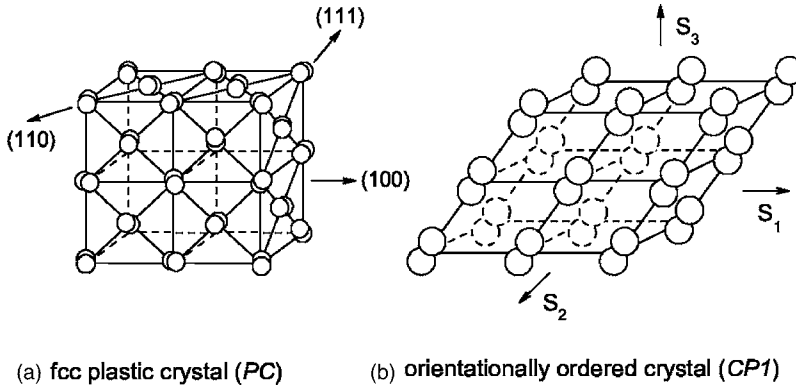


FIG. 1. A schematic picture showing the two hard-dumbbell crystal structures: (a) fcc plastic crystal; (b) orientationally ordered crystal CP1.

a site-site hard-sphere potential with the dumbbell sphere diameter  $\sigma$ . The hard-dumbbell system is characterized by a dimensionless reduced parameter  $L^* = L/\sigma$ , where  $L$  is the bond length [28]. A crystal-melt interface can be created by the following cleaving procedure [22,25]: stage 1, cleave the crystal phase with the cleaving walls; stage 2, cleave the melt phase in a similar way; stage 3, juxtapose the cleaved crystal and melt systems by rearranging the boundary conditions while maintaining the cleaving walls; stage 4, remove the cleaving walls from the combined system. The cleaving-wall potential  $\phi_c(r)$  is taken as a short-range repulsive potential similar to the system potential. The interfacial free energy  $\gamma$  is the reversible work needed in the process divided by the area of created interface. Traditionally the total reversible work is computed by the thermodynamics integration method [20–24]. However, there exists a large hysteresis between the forward and reverse paths with a traditional thermodynamic integration method for a highly repulsive cleaving potential.

Recently, Jarzynski shows that an equilibrium free-energy difference can be expressed as an exponential average of the works performed on the system [32]:  $\exp(-\beta\Delta F) = \langle \exp(-\beta W_{i \rightarrow f}) \rangle_i$ , where  $\beta = 1/kT$  is the reciprocal temperature in energy units, and  $\Delta F = F_f - F_i$  is the free-energy difference between the initial and final equilibrium system states.  $W_{i \rightarrow f}$  is the work involved in a process taking the system from the initial to the final state. The angular brackets indicate that this quantity is an ensemble average performed on the initial equilibrium system state “ $i$ .” This result is independent of both the path from the initial to the final system state and the rate of system parameters changing along the path, which suggests that the equilibrium free-energy difference can be extracted directly from an ensemble of nonequilibrium works. Thus, instead of computing the reversible work with a thermodynamic integration method, we can obtain the free-energy difference by the nonequilibrium work measurements [25]. However, straightforward employment of Jarzynski equality is impractical, especially for the cases where the free-energy difference between two equilibrium states is relatively large. In order to circumvent such difficulties, the multiple-step thermodynamic perturbation strategy may be the best choice as we demonstrated recently [25]. Moreover, the Bennett acceptance ratio method [33,34] is used to minimize the variance in the calculation of the free-energy difference between two equilibrium states by combining the information in both forward and reverse paths [34,25].

In this work, we have calculated the crystal-melt interfacial free energies of the hard-dumbbell systems near the triple point along  $L^*$  using Monte Carlo (MC) simulations via the above strategy. First of all, the pure crystals and their melts are prepared separately according to the coexistence conditions. The coexistence densities of crystals and fluids are taken from (Ref. [29]). Details of system geometries of crystal bulk phases for different crystal orientations are given in Table I. The corresponding liquid phase has the same number of particles.

In our simulations, the principle of determining the initial and final positions of the cleaving walls  $x_i$  and  $x_f$  is that  $x_i$  should be large enough to ensure that the cleaving walls do not interact with the system, and  $x_f$  should be chosen where the molecules do not pass and collide across the cleaving plane. The forward direction of the nonequilibrium work measurements is defined as from  $x_i$  to  $x_f$ .

A series of thermodynamic perturbation steps are employed to calculate the free-energy difference for each stage in the cleaving procedure. For each thermodynamic perturbation step, the nonequilibrium works in both forward and reverse paths are sampled and then combined together to calculate the free energy difference in the corresponding perturbation step [25]. In current work, 30 000 MC steps for stages 1,2 and 50 000 MC steps for stage 4 are performed for system equilibration; 50 000 MC steps are performed for data collection for each thermodynamic perturbation step.

TABLE I. The system geometries and the number of particles of the crystal bulk phases for different crystal orientations in our simulations. For PC structures, the lengths are in units of  $a = (4/\rho_c)^{1/3}$ , which is the size of the corresponding fcc unit cell and  $\rho_c$  is the corresponding coexistence solid density. For the CP1 structure, a monoclinic form with  $\alpha = 60.0$ ,  $\beta = \gamma = 67.0$ , and the dimensions are shown with all lengths in units of  $\sigma$ , which is the diameter of the sphere of the hard-dumbbell molecules.

Solid	Interface	Geometry	Particles number
PC	(100)	$20a \times 9a \times 9a$	6480
PC	(110)	$12\sqrt{2}a \times 6\sqrt{2}a \times 9a$	5184
PC	(111)	$12\sqrt{3}a \times 5.5\sqrt{2}a \times 3\sqrt{6}a$	4752
CP1	$S_1$	$32.56\sigma \times 16.28\sigma \times 13.88\sigma$	4500
CP1	$S_2$	$32.58\sigma \times 16.29\sigma \times 13.91\sigma$	4500
CP1	$S_3$	$33.35\sigma \times 16.28\sigma \times 16.28\sigma$	5400

TABLE II. The crystal-melt interfacial free energies of different crystal orientations of the hard-dumbbell systems. All interfacial free energies are in units of  $k_B T/d^2$ , where  $d$  is the diameter of a hard sphere with the same volume as the hard dumbbell and  $d^3 = \sigma^3(1 + \frac{3}{2}L^* - \frac{1}{2}L^{*3})$ . The interfacial free energies along  $S_1$  and  $S_2$  are the same due to symmetry.

Solid	$L^*$	$\gamma_{100}$	$\gamma_{110}$	$\gamma_{111}$
PC	0.0	$0.59 \pm 0.01$	$0.58 \pm 0.01$	$0.57 \pm 0.01$
	0.15	$0.57 \pm 0.01$	$0.57 \pm 0.01$	$0.57 \pm 0.01$
	0.30	$0.60 \pm 0.01$	$0.60 \pm 0.01$	$0.60 \pm 0.01$
		$\gamma_{S_1}$	$\gamma_{S_2}$	$\gamma_{S_3}$
CPI	0.40	$2.19 \pm 0.02$	$2.19 \pm 0.02$	$2.48 \pm 0.02$

Nonequilibrium works are sampled at every configuration during the run of data collection.

Actually, the number of thermodynamic perturbation steps needed in each stage depends not only on the free-energy difference between initial and final states, but also on the system potential. In practice, it is straightforward to determine the number of thermodynamic perturbation steps according to the Bennett variance. Namely, if the Bennett variance becomes very large in certain thermodynamic perturbation steps, an intermediate state should be inserted to improve the accuracy of the result. Thus, we can flexibly design a scheme of calculating the free-energy difference to make the calculations more efficient and accurate for various systems.

The interfacial free energies of different crystal orientations for the hard-dumbbell systems are obtained by summing the free-energy differences in the four stages. For the hard-dumbbell system, there is no work required in stage 3. The results are scaled with the diameter of a hard sphere with the same volume as the hard dumbbell and given in Table II. Our estimate of error bars includes two parts: statistical and systematic errors. The statistical error can be reduced by increasing the number of thermodynamic perturbation steps and the sampling number of nonequilibrium works. The main systematic error results from the fluctuations of the interface position. When the cleaving walls are far from the cleaving plane, the position of the interface cannot be confined at the cleaving plane exactly, especially in stage 4 where the system contains two interfaces. In order to estimate the systematic errors, several independent computations for stage 4 with different perturbation step sizes are performed and the largest variance is taken as a systematic error. Compared with statistical error, the systematic error is more important in the current case. The combinations of statistical and systematic errors are given in Table II as total error bounds.

As the plastic crystal phase of a hard-dumbbell system is equivalent to an effective fcc hard-sphere system, the scaled interfacial free energy of a plastic crystal phase would be expected to be the same as that of the hard-sphere system. In fact, from the results shown in Table II, it can be seen that the scaled interfacial free energies of the PC phase do not change much with the reduced bond length  $L^*$  even when there are substantial coexistence density changes. Moreover, the anisotropy of the interfacial free energies of PC hard-

dumbbell systems disappears within our error estimate as  $L^*$  increases. This is due to the fact that the differences among the interfaces of different crystal orientations are greatly weakened by the orientational disorder of hard-dumbbell molecules. Once the orientations of the hard-dumbbell molecules become ordered, the interfacial free energies increase dramatically, which are more than three times larger than that of an orientationally disordered PC phase [35]. In addition, the anisotropy of the interfacial free energies of a CPI phase is about 13% which is an order of magnitude larger than the estimate in metallic systems [7], where 1–2 % anisotropy is already known to affect solidification significantly.

Such large increases both in the magnitude and in anisotropy of the interfacial free energies for the orientationally ordered phase may have significant implications in our understanding of the nucleation processes of molecular systems. Assuming that this trend does not change dramatically when soft attractions are added to the system, which is true for isotropic systems [24], we would expect that the formation of an orientationally ordered crystal phase will be significantly difficult and a nonspherical critical nucleus path may be the rule rather than the exception. It will be interesting to see how the strength and range of soft attractions can affect the interfacial free energies in anisotropic systems, especially when the critical point becomes metastable [26].

In summary, we have calculated the crystal-melt interfacial free energies of different crystal orientations for the hard-dumbbell systems near the triple point along  $L^*$  directly using a multistep thermodynamic perturbation method by nonequilibrium work measurements with a cleaving procedure. We find that for the plastic crystal phase, the interfacial free energy  $\gamma$  decreases with the reduced bond length  $L^*$  increasing and the anisotropy disappears. With the ordering of the orientations of the hard-dumbbell molecules, the interfacial free energy  $\gamma$  increases dramatically and the anisotropy becomes an order of magnitude stronger in contrast to the isotropic systems.

In contrast to the traditional thermodynamic integration method, the efficiency and reliability of the multistep thermodynamic perturbation method makes the calculations possible. For example, in the stage 2 of the splitting liquid system, additional stretching and compressing of the liquid system are needed in order to avoid a large hysteresis of the reversible work for the thermodynamic integration method [24]. For the multistep thermodynamic perturbation method,

the free-energy difference in each stage can be directly computed without any other additional modifications. Furthermore, since the free-energy difference is obtained by non-equilibrium work measurements and a combination of the information from both the forward and reverse paths minimizes the statistical error, there is no requirement on the reversibility of the path and no hysteresis in the calculations. Therefore, this method will be very useful for the calculations of free-energy differences, especially for those situations where it is difficult to use thermodynamic integra-

tion due to the large hysteresis between the forward and reverse paths. Our applications to the dumbbell system offer an example where such calculations will not be practical otherwise.

#### ACKNOWLEDGMENTS

The authors are grateful for the financial support from a NSF Grant No. CHE0303758.

- 
- [1] W. A. Tiller, *The Science of Crystallization: Microscopic Interfacial Phenomena* (Cambridge University Press, New York, 1991).
- [2] D. Turnbull, *J. Appl. Phys.* **21**, 1022 (1950).
- [3] C. Smits, J. S. van Duijneveldt, J. K. G. Dhont, H. N. W. Lekkerkerker, and W. J. Briens, *Phase Transitions* **21**, 157 (1990).
- [4] S. M. Underwood, J. R. Taylor, and W. van Meegen, *Langmuir* **10**, 3550 (1994).
- [5] D. W. Marr and A. P. Gast, *Langmuir* **10**, 1348 (1994).
- [6] M. E. Glicksman and C. Vold, *Acta Metall.* **17**, 1 (1969).
- [7] R. E. Napolitano, S. Liu, and R. Trivedi, *Interface Sci.* **10**, 217 (2002).
- [8] W. A. Curtin, *Phys. Rev. Lett.* **59**, 1228 (1987).
- [9] D. W. Marr and A. P. Gast, *Phys. Rev. E* **47**, 1212 (1993).
- [10] R. Ohnesorge, H. Lowen, and H. Wagner, *Phys. Rev. E* **50**, 4801 (1995).
- [11] V. B. Warshavsky and X. Song, *Phys. Rev. E* **73**, 031110 (2006).
- [12] J. J. Hoyt, M. Asta, and A. Karma, *Phys. Rev. Lett.* **86**, 5530 (2001).
- [13] J. J. Hoyt, M. Asta, and A. Karma, *Mater. Sci. Eng., R.* **41**, 121 (2003).
- [14] E. Chacón and P. Tarazona, *Phys. Rev. Lett.* **91**, 166103 (2003).
- [15] J. R. Morris, Z. Y. Lu, Y. Y. Ye, and K. M. Ho, *Interface Sci.* **10**, 143 (2002).
- [16] J. R. Morris, *Phys. Rev. B* **66**, 144104 (2002).
- [17] J. R. Morris and X. Song, *J. Chem. Phys.* **119**, 3920 (2003).
- [18] Y. Mu, A. Houk, and X. Song, *J. Phys. Chem. B* **109**, 6500 (2005).
- [19] Xiaobing Feng and B. B. Laird, *J. Chem. Phys.* **124**, 044707 (2006).
- [20] J. Q. Broughton and G. H. Gilmer, *J. Chem. Phys.* **84**, 5759 (1986).
- [21] R. L. Davidchack and B. B. Laird, *Phys. Rev. Lett.* **85**, 4751 (2000), and references therein.
- [22] R. L. Davidchack and B. B. Laird, *J. Chem. Phys.* **118**, 7651 (2003).
- [23] R. L. Davidchack and B. B. Laird, *Phys. Rev. Lett.* **94**, 086102 (2005).
- [24] R. L. Davidchack and B. B. Laird, *J. Phys. Chem. B* **109**, 17802 (2005).
- [25] Y. Mu and X. Song, *J. Chem. Phys.* **124**, 034712 (2006).
- [26] X. Song, *Phys. Rev. E* **66**, 011909 (2002).
- [27] S. T. Yau and P. G. Vekilov, *Nature (London)* **406**, 494 (2000).
- [28] C. Vega, E. P. A. Paras, and P. A. Monson, *J. Chem. Phys.* **96**, 9060 (1992).
- [29] C. Vega, E. P. A. Paras, and P. A. Monson, *J. Chem. Phys.* **97**, 8543 (1992).
- [30] H. J. Woo and X. Song, *Phys. Rev. E* **63**, 051501 (2001).
- [31] H. J. Woo and X. Song, *J. Chem. Phys.* **116**, 4587 (2002).
- [32] C. Jarzynski, *Phys. Rev. Lett.* **78**, 2690 (1997).
- [33] C. H. Bennett, *J. Comput. Phys.* **22**, 245 (1976).
- [34] D. Frenkel and B. Smit, *Understanding Molecular Simulation: From Algorithms to Applications* (Academic Press, San Diego, 1996).
- [35] Brian Laird (private communications). If scaled with coexistence pressure, the average interfacial free energies of the OOC phase are about two times larger than that of an orientationally disordered PC phase:  $\bar{\gamma}^*/P^*$  of an OOC phase with  $L^*=0.40$  and a PC phase with  $L^*=0.30$  are 0.0634 and 0.0343, respectively, where  $\bar{\gamma}^*$  is defined as  $\beta\bar{\gamma}d^2$  and  $P^*=\beta Pd^3$  is the reduced coexistence pressure. This clearly shows that the increase on the interfacial free energy from a PC phase to an OOC phase due to the change of crystal structure is dramatically larger than the expected change due to the change of coexistence density. Our preliminary results for  $L^*=0.6$  also confirm the above trend.